EXPERIMENTAL SELF–SENSING RESULTS FOR A MAGNETIC BEARING

Dominick Montie
Department of Mechanical and Aerospace Engineering, University of Virginia, Charlottesville, Virginia, dtm7e@virginia.edu
Eric Maslen
Department of Mechanical and Aerospace Engineering, University of Virginia, Charlottesville, Virginia, ehm7s@virginia.edu

ABSTRACT

Experimental results are presented for a self-sensing magnetic bearing system operated in both the linear and saturation regions. When the magnetic actuator operates exclusively in the linear region, a simple, inexpensive analog estimation technique is implemented. When operating conditions are expected to drive the bearing into magnetic saturation, a digital-analog hybrid estimator is introduced. It follows that expected operating conditions of the magnetic bearing system determine the necessary complexity of the position estimator. Further, the performance of the analog hardware plays a critical role in the operation of the estimator from the perspective of signal gain and phase. Such hardware issues, as they relate to estimator performance, are discussed. Recommendations for improved estimator performance in conjunction with reduced estimator cost and complexity follow.

INTRODUCTION

A primary motivation for the use of self-sensing in magnetic bearings [1, 3, 4, 5] is the elimination of discrete position sensors, the advantages of which have been enumerated many times before. However, a primary impediment to its implementation is the apparent lack of robustness and relatively poor performance achieved through linear observer-based solutions. This issue is explored at a fundamental level by Morse, et al [6] who demonstrated that for linear systems, the robustness properties can never match those obtained with a discrete position sensor. In that work, it was shown that, for a linearized magnetic bearing system in conjunction with a linear controller, the gain and phase margins of a self-sensing scheme can be more than two orders of magnitude smaller than for a position-measured system (depending on the system physical parameters).

In the present work, a nonlinear filter is embedded in a parameter estimation-based technique for extracting rotor position from bearing amplifier signals, as described in [1]. It is suggested that this technique effectively sidesteps the fundamental limitations discussed in [6] and the experimental results presented here appear to support this. This relationship between performance bounds for a linear system and for the current nonlinear system is a point of future research.

The results presented in this paper demonstrate progress in the performance of self–sensing and point to directions in which substantially more progress can be made. Experimental transient and steady–state performance results are evaluated for a rigid rotor system, with emphasis on bandwidth, tracking error, gain margin, and noise. These results are provided for self–sensing applied to one and both axes of one bearing in the magnetically unsaturated region (using the fully analog estimator) and for self–sensing along one axis subject to bearing saturation (using a digital weighting algorithm in conjunction with the analog estimator) under forcing conditions due to levitation controller disturbance injection and high speed rotor spin.

The following sections include a discussion of the parameter estimator used, the theoretical basis for the inductor model in the estimator, and a description of the experimental results obtained. Following this is a discussion of methods for improving performance while decreasing system cost and complexity. The paper concludes with some summary remarks on the current state of our experimental work and a look toward future research.

PARAMETER ESTIMATOR

The parameter estimator employed in this paper is based on the one described in [1]. It consists of a linear inductor model, a pair of nonlinear current filters, and a PI posi-

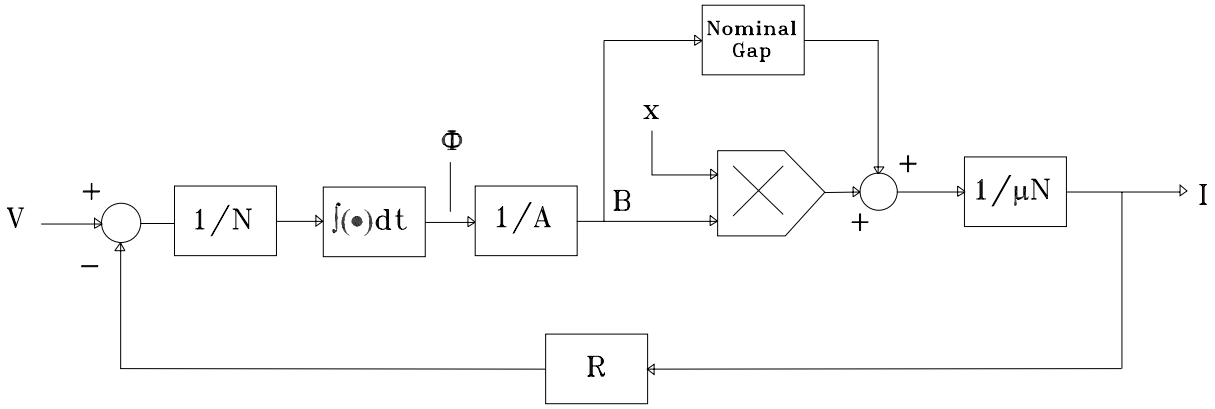

FIGURE 1: Diagram of Analog Inductor Model

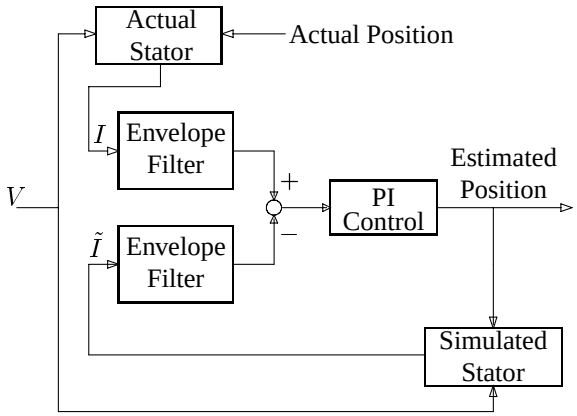

FIGURE 2: Diagram of Estimation Scheme

tion convergence controller (Figure 2), all implemented with analog electronics. The inductor model used here differs from that used in [1] in that it is derived with respect to the magnetic flux rather than from a more common inductance argument. The model is derived from a combination of Ohm's and Faraday's laws:

$$V(t) - i(x,t)R = N\frac{\partial \phi(x,t)}{\partial t}$$

which produces, by simple integration,

$$\phi(x,t) = \int_0^t \frac{1}{N}(V(\tau) - i(x,\tau)R)d\tau$$

Using Ampére's loop law:

$$\mathcal{R}(x,t)\phi(x,t) = Ni(x,t)$$

and combining, gives:

$$i(x,t) = \frac{\mathcal{R}(x,t)}{N^2}\int_0^t (V(\tau) - i(x,\tau)R)d\tau$$

where $\phi(x,t)$ is the magnetic flux, $V(t)$ is the applied coil voltage, $i(x,t)$ is the coil current, $\mathcal{R}(x,t)$ is the magnetic reluctance, R is the resistance of the coil pair, and N is the number of turns in the coil pair. A diagram of the analog implementation of these equations is illustrated in Figure 1.

This model offers a number of advantages over the direct inductance-based model used in [1]. For instance, in the technique used in [1], it is necessary to ignore the effects of rotor velocity-induced back-EMF, while in the formulation described above it is not. The derivation of the current via the equation for the magnetic flux has the advantage that there are as few simplifying assumptions as possible (the most important one being the assumption of no mutual inductance between coil pairs). Furthermore, as demonstrated in Figure 1, there are signals that are available in this circuit that are valuable for other reasons. For instance, the signal proportional to magnetic flux might be used to operate the switching amplifiers under flux feedback, instead of current feedback. Advantages to this approach include minimizing sensitivity to magnetic nonlinearities and the open–loop stiffness that is inherent in using current control in the switching amplifiers.

EXPERIMENTAL RESULTS

Experimental Apparatus

The experimental test rig used for this paper consisted of two radial bearings, one thrust bearing, and a short (essentially rigid) rotor spun by an air turbine. The self-sensing technique was applied to one radial (symmetric, eight-pole, silicon iron) bearing whose adjacent poles are wound in reverse series (i.e., 2 opposing "horseshoes" along horizontal and vertical axes). The relevant parameters of the radial magnetic bearings are a nominal gap length of 0.5 mm, a pole face cross-sectional area of 108 mm^2, 140 coil turns per pole pair, a rotor diameter of 38 mm, and bias current of 2A. Rotor position was measured directly using Bently Nevada eddy current probes with a gain of 8 V/mm. The controller was configured to accept as its rotor position input either the signal from the eddy current probes or from the position estimators,

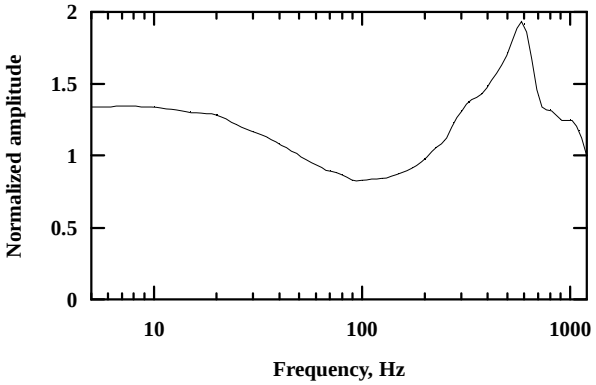

FIGURE 3: Normalized Frequency Response of the Estimator

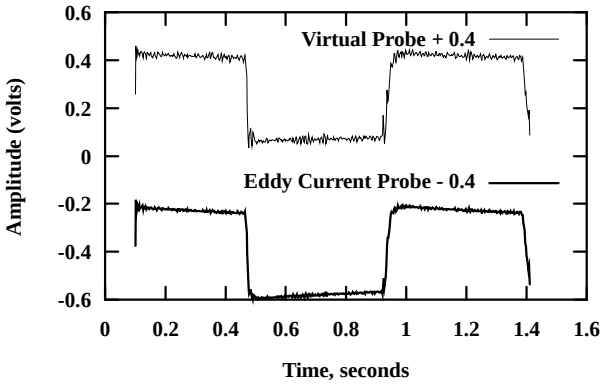

FIGURE 5: Step Response of the Position Estimator

selectable by a mechanical switch.

Linear Regime Tests

For operation in the linear region, a fully analog parameter estimator is implemented. The basis for the analog estimator operation with an unsaturated bearing is the linear relationship between the demodulated bearing current signal (internal to the estimator) and rotor position. Thus, in the linear region, only one coil pair of either axis is required to estimate position.

The first test performed was for self–sensing along one axis only. The data from this test, shown in Figure 3, was obtained by introducing a sine wave disturbance into the digital levitation controller reference position input. The bearing current was used by the digital controller to drive this apparent rotor displacement to zero, thus actually displacing the rotor sinusoidally 180° phase-shifted from the reference input (see Figure 4).

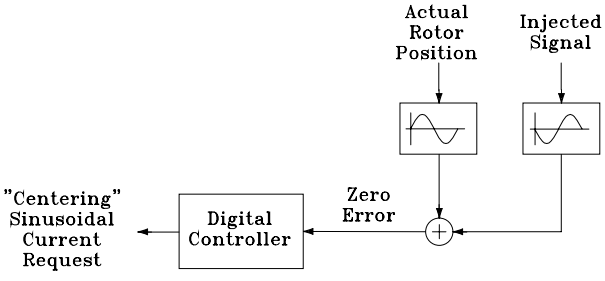

FIGURE 4: Point of Perturbation Signal Injection

The magnitude plot demonstrates a strong correlation between actual probe position signal and virtual probe (sensed position) signal over a large frequency range. The linear magnitude scale is used for greater data resolution; when plotted on a log-log scale (as are most performance plots), there would be very little sensitivity of gain to frequency.

The variation in gain over the frequency range appears to be correlated to the structural resonance of the test rig, which increases the sensitivity of estimator output to force variation and has the effect of increasing the magnitude of the estimated position. While this effect has not been fully investigated, it appears to be the cause of the peak at 600Hz. The rolloff at high frequency is expected; the convergence controller has a finite bandwidth, as do the envelope filters.

In Figure 5, the transient behavior of the virtual probe is demonstrated. This response was obtained by injecting a square wave disturbance into the digital levitation controller reference input, with the rig supported along the axis of interest using the virtual probe. While the signal is too noisy to resolve any ringing in the estimation directly after a switch, there is no discernible overshoot, ringing, or difference in response time constant.

For the spin test, an air turbine attached to the rotor was used to spin the rotor up to 60,000 RPM (1 kHz), with both axes of a single bearing supported with self-sensing. Rotor displacement was caused by rotor unbalance and imperfect coupling between the rotor and motor. Thus, as rotor speed increased, unbalance response increased. However, the rotor displacement was not so large as to drive the bearing into magnetic saturation. The eddy current probe output (when the rotor was levitated using the virtual probes) is shown in Figure 6. For purposes of clarity, the comparison between the two displacement signals (actual and virtual for one axis only) are made with a normalized power spectrum (Figure 7).

It is clear from Figure 6 that there is a strong effect of low frequency structural resonances on the estimator output, demonstrated by the 1 kHz signal superposed on a signal of lower frequencies. Furthermore, the superharmonic content of the virtual probe is much larger than that of the eddy current probe, as seen in Figure 7. Nevertheless,

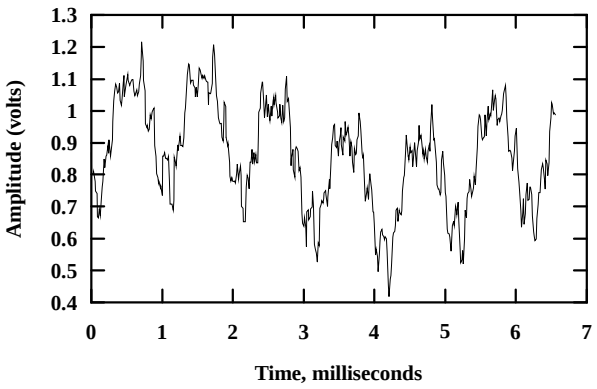

FIGURE 6: Eddy Current Probe Output with Rotor at 60,000 RPM

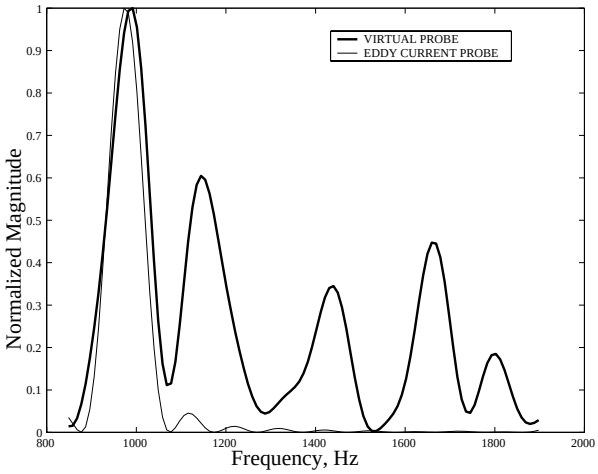

FIGURE 7: Comparison of High-Frequency Power Spectra with Rotor at 60,000 RPM

the important characteristics present in the actual probe response are also present in that of the virtual probe; the necessary estimator gain and phase margins were present for successful levitation out to 1kHz. Furthermore, circuit design and modeling improvements discussed later, which promise to improve estimator accuracy and bandwidth, should at the same time decrease harmonic content and improve position resolution.

The final criterion used to evaluate the performance of the estimator is the gain margin comparison between actual and virtual probes. In this test, the digital controller gain was varied to determine the range over which the closed loop system remained stable. It is important to note that the same controller was used for both the eddy current probe (actual probe) and the estimated signal (virtual probe). Using the actual probes, the gain range that stabilized the rotor is 0.4 to 3.5 (variations on the nominal controller gain), while for the virtual probes the stabilizing gain range is 0.4 to 1.1. This loss in upper gain range is expected since the virtual probe has nearly twice the gain of the eddy current probe at 600 Hz. Thus, for comparison, scale the upper gain limit of 1.1 by the probe gain at 600 Hz of 2.0 to obtain a gain range of 0.4 to 2.2.

Magnetic Saturation Regime Tests

The relationship between switching ripple amplitude and rotor position becomes both nonlinear and multi-valued when the magnetic bearing is operated in the saturation region. Since the parameter estimator employed here may converge to the incorrect branch of this multi-valued position relationship as a result of the linear inductor model used, additional information is required. When the magnetics are saturated, information from both opposing coil pairs is required to ensure proper position convergence. Thus, for actuator operation into magnetic saturation, a digitally-implemented estimator output weighting algorithm is employed.

When the bearing magnetics become saturated, the linear inductor model fails to adequately map input voltage and position to current, and the estimator performance is poor. For instance, at high frequencies and large displacements, each side of one axis will be saturated for approximately half of one cycle (when the levitation controller commands large currents to provide a restoring force of sufficient magnitude on the displaced rotor). An example of an estimated displacement when a large amplitude, high frequency (200Hz) disturbance signal is introduced into the levitation controller is shown in Figure 8. For almost one half-cycle the signal is approximately sinusoidal, but is highly distorted during the other half-cycle.

This leads to the theoretical basis for the technique implemented for a saturated bearing: use only the unsaturated position estimate from each set of coil pairs for a single axis. Thus, a parameter estimation circuit was constructed for each of the opposing pole pairs along one axis. Then, in the digital levitation controller, a selection algorithm was used to weight and combine the two virtual probe signals for use as a position estimate. For each control loop, the digital controller would calculate the magnitude of the perturbation current (I_{pert}). If the magnitude of this value was greater than a specified threshold T_{pert}, only one or the other estimated position signal was used (e.g., x_{pos} or $-x_{neg}$, whichever corresponded to an unsaturated pole pair). If I_{pert} was below this bound, a linear weighting algorithm was employed:

$$\begin{aligned} x_{weighted} &= C(T_{pert} + I_{pert})x_{pos} \\ &\quad -C(T_{pert} - I_{pert})x_{neg} \end{aligned}$$

where $C = 0.5/T_{pert}$. To avoid cross-over discontinuity (and the fine calibration necessary to minimize it) a

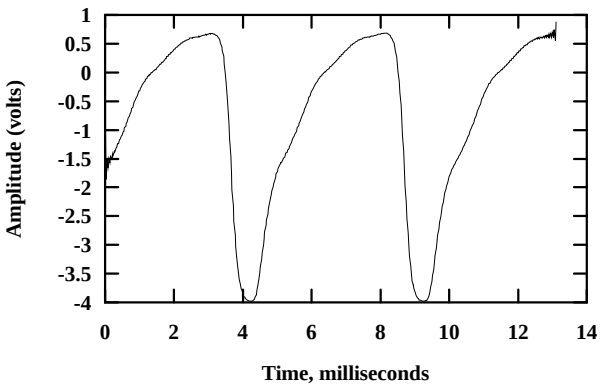

FIGURE 8: Linear Estimator Output Subject to Magnetic Saturation

simple binary selection algorithm was not used (an issue also addressed in [2]).

Using this technique, the performance was significantly lower than for the unsaturated case. Levitation could only be achieved for frequencies up to about 200 Hz, and even at these low frequencies stability was marginal. The position estimation was poor enough that the apparent controller stiffness was significantly decreased, allowing large-amplitude rotor position errors. This loss of performance was most likely caused by the fact that for part of the unsaturated half-cycle, the position estimate contains enough distortion of the sinusoidal signal (held over from a lagging response in the estimator, which must recover from the transients introduced by the saturation) that switching between the two "unsaturated" estimator half-cycles still produces poor performance. A method of implementing circuitry which includes a saturation model is proposed in [2].

ACHIEVING IMPROVED PERFORMANCE

One avenue for improving position estimation is increasing the internal signal-to-noise ratio of the estimator. Presently, the analog electronics model the full current signal (DC bias, AC perturbation, and switching effect). For this bearing model, the output current is always positive (as it is in the actual bearing, since requested bearing currents are clipped at zero in the digital levitation controller). Thus, for the signals in the analog circuitry, an achievable +/- 10V signal range is limited to, at most, 0-10V. However, in order to achieve an acceptable signal-to-noise ratio for the entire current signal (DC, AC, and switches), 1A in the bearing was modeled by 1V in the circuit. A better technique would be to model the current by separating its components - DC, and AC and switching effects - into different circuits. In this way, the signal gains from the current sensors in the switching amplifiers and those in the estimation loop could be increased to their maximum achievable levels.

There are two analog components that contribute to force feed–through: the envelope filters and the inductor model. If both the filters and inductor model could be made exact, the same voltage input to the actual and simulated system (at a fixed, centered rotor position) would yield the same outputs, eliminating any effect of force feed–through. Thus, the combination of a more exact inductor model (one which includes nonidealities) and more closely matched filters would significantly reduce this effect. Based on experience, it is not difficult to match filters closely. Therefore, the effect of filter unmatch on estimator performance (e.g., the rotor stability problems encountered by the gain and phase errors introduced by force feed-through) will not be an issue in the future. However, the filter design can still be improved in such a way to make filter matching trivial. Some improvements include eliminating unnecessary components and filter stages, simplifying circuit layout, combining redundant functions, and replacing current stages with superior components which reduce signal distortion and increase signal gain. These changes will have the effect of reducing some signal noise, reducing component count and cost, and shrinking the electronics package.

Significantly greater errors which degrade estimator performance are introduced through an imperfect analog inductor model. While it is much harder to match the inductor model to the actual bearing characteristics than it is to match the two envelope filters, a correspondingly more significant improvement in estimator performance can be achieved. While a digital–analog hybrid technique was implemented here for a quick study of its potential usefulness, a complete nonlinear inductor model is a more realistic (and certainly more practical) alternative in terms of cost and complexity. The primary phenomena not modeled here are magnetic saturation, hysteresis, and eddy currents. The first two have been relatively unimportant under normal operating conditions because the coil currents and rotor displacement are limited in such a way that their effects are negligible. The final phenomenon, however, is present under all operating conditions. By including such non–ideal effects, the performance hit incurred due to the nonlinear effects present in the "unsaturated" half-cycles described earlier will be minimized.

CONCLUSIONS

Though research has been published describing inferior performance limits of a linear self-sensing system, the nonlinear signal processing incorporated in the present technique appears to exclude this estimation scheme from such limitations. Furthermore, it is proposed that the robustness of such a self-sensing scheme is limited only by the accuracy of the inductor model and performance of the parallel filters and convergence controller,

while the performance is also a function of bearing design. The examination of performance limits for the nonlinear technique used is an important topic of further study, as is how the performance limits compare to those developed for a fully linear system.

This paper also included a discussion of results for a self-sensing magnetic bearing which demonstrate progress toward realizing a viable alternative to discrete position sensors. The experimental results obtained thus far suggest that this parameter estimation technique has the potential for success. It is clear that the performance obtained so far is significantly inferior to that of discrete position sensors. However, the progress made with the current system lends merit to the argument that with a more complete inductor model and circuitry that enhances the estimator's signal-to-noise ratio, a high-performance self-sensing technique is achievable. These plans for specific improvements in estimator design directly precede a complete series of experimental tests to fully characterize system performance in light of published performance limitations.

References

[1] Noh, M. D., *Self-Sensing Magnetic Bearings Driven by a Switching Power Amplifier.* Ph.D. Dissertation, University of Virginia, 1996.

[2] Noh, M. D., and Maslen, E. H., "Self–Sensing Magnetic Bearings (Part II): Effects of Saturation," in Proceedings of the Fifth International Symposium on Magnetic Bearings, Kanazawa, Japan, August 1996, pp. 113–118.

[3] Iannello, V., *Sensorless Position Detector for an Active Magnetic Bearing*. U.S. Patent No. 5,696,412, Dec. 9, 1997.

[4] Mizuno, T., Bleuler, H., Gähler, C., Vischer, D., "Towards Practical Applications of Self-Sensing Magnetic Bearings," *Proceedings of the Third International Symposium on Magnetic Bearings.* Alexandria, Virginia, August, 1992, pp. 169–175.

[5] Vischer, D., and Bleuler, H., "A New Approach to Sensorless and Voltage Controlled AMBs Based on Network Theory Concepts," *Proceedings of the Second International Symposium on Magnetic Bearings*, Tokyo, July 12-14, 1992, pp. 301–306.

[6] Morse, N., Smith, R., Paden, B., Antaki, J., "Position Sensed and Self-Sensing Magnetic Bearing Configurations and Associated Robustness Limitations," Proceedings of the IEEE Conference on Decision and Control Including the Symposium on Adaptive Processes. v 3 1998. p 2599-2604